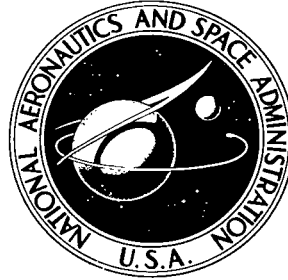


NASA
TN
D-4839
pt.2
c.1

NASA TECHNICAL NOTE



NASA TN D-4873

NASA TN D-4873



LOAN COPY: RET
AFWL (WLIL
KIRTLAND AFB, N MEX

INCOMPRESSIBLY LUBRICATED RAYLEIGH STEP JOURNAL BEARING

II — Infinite-Length Solution

by Bernard J. Hamrock and William J. Anderson

Lewis Research Center

Cleveland, Ohio



INCOMPRESSIBLY LUBRICATED RAYLEIGH STEP JOURNAL BEARING
II - INFINITE-LENGTH SOLUTION

By Bernard J. Hamrock and William J. Anderson

Lewis Research Center
Cleveland, Ohio

NATIONAL AERONAUTICS AND SPACE ADMINISTRATION

For sale by the Clearinghouse for Federal Scientific and Technical Information
Springfield, Virginia 22151 - CFSTI price \$3.00

ABSTRACT

A theoretical analysis of pressure distribution, load capacity, attitude angle, and friction force was performed for an eccentric Rayleigh step journal bearing with varying numbers of steps and infinite length. The results indicated that one step placed around the journal was optimal. For small eccentricity ratios the optimal film thickness ratio was 1.7, while there were three optimal ratios of the angle subtended by the ridge to the angle subtended by the pad of 0.4, 0.45, and 0.5. These ratios depend on whether load capacity, or stability, or both load capacity and stability is more important in the application being considered.

INCOMPRESSIBLY LUBRICATED RAYLEIGH STEP JOURNAL BEARING

II - INFINITE-LENGTH SOLUTION

by Bernard J. Hamrock and William J. Anderson

Lewis Research Center

SUMMARY

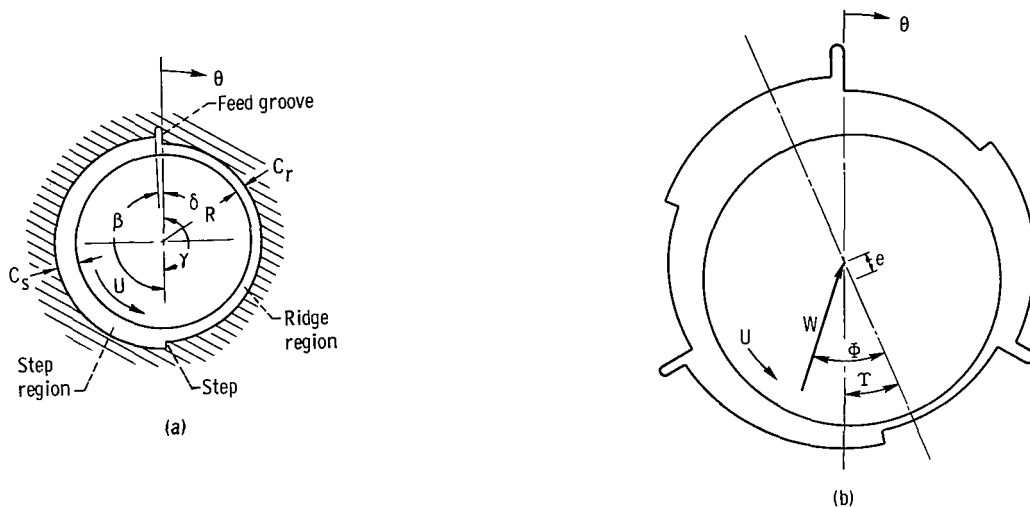
A theoretical analysis of pressure distribution, load capacity, attitude angle, and friction force for an eccentric Rayleigh step journal bearing with varying number of steps and infinite length was performed. The analysis was broken into two parts: the ridge region and the step region. The pressure distribution in the respective ridge or step region was obtained from the Reynolds equation which neglects the side leakage term. Once the pressure is known, the load components, the attitude angle, and the friction force can be derived. The resulting equations were determined to be a function of the eccentricity ratio ϵ , the eccentricity orientation angle Υ , the number of steps placed around the journal N , the step to ridge film thickness ratio k , the ratio of the angle subtended by the ridge to the angle subtended by the pad ψ , and the angle subtended by the lubrication groove δ . The results are valid only for the radius to length ratio of zero, since the side leakage term of the Reynolds equation was neglected in the analysis. The results, however, are applicable for the entire range of eccentricity ratio ($0 \leq \epsilon < 1$).

The resulting expressions for dimensionless pressure, load, friction, and attitude angle were evaluated on a digital computer. The results indicated that one step placed around the journal was optimal. For eccentricity ratios greater than or equal to 0.2, the maximum load occurred for a bearing without a step, or a Sommerfeld bearing. For eccentricity ratios less than 0.2 the optimal film thickness ratio was 1.7, while there were three optimal ratios of the angle subtended by the ridge to the angle subtended by the pad of 0.4, 0.45, and 0.5. These ratios depend on whether load capacity, or stability, or both load capacity and stability is more important in the application being considered. It also was determined from the pressure profiles for the various eccentricity ratios that regardless of the eccentricity orientation angle, the optimal Rayleigh step journal bearing has characteristics superior to those of the conventional Sommerfeld bearing.

INTRODUCTION

The reasons for investigating a Rayleigh step journal bearing, as well as a detailed historical background, are given in reference 1. The historical background describes the work of Lord Rayleigh (ref. 2), Archibald (refs. 3 and 4), and others on the subject of Rayleigh step bearings. In reference 1 the concentric Rayleigh step journal bearing was investigated. Because of the assumption of concentricity of journal and bearing, the number of steps placed around the bearing had to be limited to one to obtain a nonzero load capacity. The results obtained, which were valid for the entire range of radius to length ratio ζ , indicated optimal values of $k = 1.7$ and $\psi = 0.35$ for maximum load capacity.

Sketch (a) shows the concentric Rayleigh step journal with the various symbols used in the analysis. Sketch (b) indicates additional symbols for the eccentric Rayleigh step



journal. From these sketches a pad is defined as the portion of the bearing included in the angle subtended by the ridge, step, and lubrication groove. Furthermore, each pad acts independently since the pressure is reduced to ambient at the lubrication supply grooves.

This investigation was conducted to find the optimal number of steps and the step configuration for maximum load capacity and stability (as indicated by low attitude angle) for the infinite-length, incompressibly lubricated, step journal bearing.

SYMBOLS

| | |
|---------------|---|
| A, B | integration constants |
| b | constant defined in analysis |
| C | radial clearance |
| e | journal and bearing eccentricity |
| F | dimensionless friction force, $fC/2\pi R\mu U$ |
| f | friction force per unit length |
| G, g | constants defined in analysis |
| H | dimensionless film thickness, h/C |
| h | thickness of lubricating film |
| J | constant defined in analysis |
| k | film thickness ratio, C_s/C_r |
| L | length of bearing |
| N | number of steps placed around bearing |
| n | step index 1, 2, . . . , N |
| P | dimensionless pressure, $C^2(p - p_a)/6\mu UR$ |
| p | film pressure |
| p_a | ambient pressure |
| Q | volume flow rate per unit length |
| R | radius of bearing |
| r, S, s, T, t | constants defined in analysis |
| U | velocity of journal surface |
| W | dimensionless load capacity, $w/p_a R\Gamma$ |
| WR | dimensionless radial load capacity, $w_r/p_a R\Gamma$ |
| WT | dimensionless tangential load capacity, $w_t/p_a R\Gamma$ |
| w | load capacity per unit length |
| w_r | radial load capacity per unit length |
| w_t | tangential load capacity per unit length |
| β | angle subtended by step region |

- Γ dimensionless parameter, $6\mu UR/p_a C_r^2$
 γ angle subtended by ridge region
 δ angle subtended by lubrication groove
 ϵ eccentricity ratio, e/C_r
 ζ radius to length ratio, R/L
 η value of θ at ridge boundary, $2\pi(n - 1)/N$
 θ angular coordinate
 μ viscosity of fluid
 ξ value of θ at step boundary, $2\pi/N (n - \delta)$
 σ value of θ at common boundary of ridge and step, $2\pi/N (n - 1 + \psi)$
 τ shear stress
 Υ eccentricity orientation angle, angle between $\theta = 0^0$ line and line of centers of journal and bearing
 Φ attitude angle
 ψ ratio of angle subtended by ridge to angle subtended by pad, $\gamma/(\gamma + \beta + \delta)$

Subscripts:

- c common boundary location
r ridge region
s step region
 ∞ infinite-length-bearing solution

ANALYSIS

The Reynolds equations for the ridge and step regions developed in reference 1 and modified for the infinitely long bearing are

$$\frac{d}{d\theta} \left(H_r^3 \frac{dP_{r, \infty}}{d\theta} \right) = - \frac{dH_r}{d\theta} \quad (1)$$

$$\frac{d}{d\theta} \left(H_s^3 \frac{dP_{s, \infty}}{d\theta} \right) = - \frac{dH_s}{d\theta} \quad (2)$$

where

$$P_{r, \infty} = \frac{C_r^2(p_{r, \infty} - p_a)}{6\mu UR}$$

$$P_{s, \infty} = \frac{C_r^2(p_{s, \infty} - p_a)}{6\mu UR}$$

$$H_r = \frac{h_r}{C_r}$$

$$H_s = \frac{h_s}{C_r}$$

The equations for the circumferential flow rate in the ridge and step regions, as developed in reference 1, can be written as

$$Q_r = -\frac{UC_r}{2} \left(H_r + H_r^3 \frac{dP_{r, \infty}}{d\theta} \right) \quad (3)$$

$$Q_s = -\frac{UC_r}{2} \left(H_s + H_s^3 \frac{dP_{s, \infty}}{d\theta} \right) \quad (4)$$

The equations for the dimensionless film thickness in the ridge and step regions, as developed in the appendix may be written as

$$H_r = \frac{h_r}{C_r} = 1 + \epsilon \cos(\theta + \Upsilon) \quad (5)$$

$$H_s = \frac{h_s}{C_r} = k + \epsilon \cos(\theta + \Upsilon) \quad (6)$$

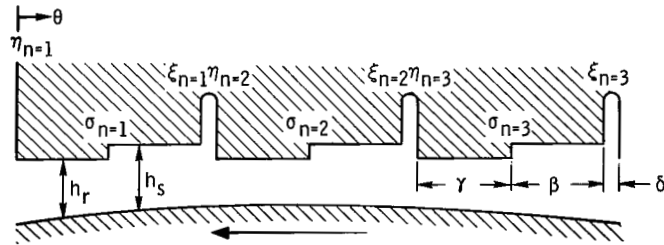
where $\epsilon = e/C_r$ and $k = C_s/C_r$.

Substitution of equations (5) and (6) into equations (1) and (2), respectively, and integrating give

$$\begin{aligned}
P_{r, \infty} = & \frac{\epsilon \sin(\theta + \Upsilon)}{(1 - \epsilon^2)[1 + \epsilon \cos(\theta + \Upsilon)]} - \frac{\cos^{-1} \left[\frac{\epsilon + \cos(\theta + \Upsilon)}{1 + \epsilon \cos(\theta + \Upsilon)} \right]}{(1 - \epsilon^2)^{3/2}} \\
& + \frac{A_r \left(1 + \frac{\epsilon^2}{2} \right)}{(1 - \epsilon^2)^{5/2}} \cos^{-1} \left[\frac{\epsilon + \cos(\theta + \Upsilon)}{1 + \epsilon \cos(\theta + \Upsilon)} \right] \\
& + \frac{A_r \epsilon \sin(\theta + \Upsilon) [\epsilon^2 - 3\epsilon \sin(\theta + \Upsilon) - 4]}{2(1 - \epsilon^2)^2 [1 + \epsilon \cos(\theta + \Upsilon)]^2} + B_r \quad (7)
\end{aligned}$$

$$\begin{aligned}
P_{s, \infty} = & \frac{\epsilon \sin(\theta + \Upsilon)}{(k^2 - \epsilon^2)[k + \epsilon \cos(\theta + \Upsilon)]} - \frac{k \cos^{-1} \left[\frac{\epsilon + k \cos(\theta + \Upsilon)}{k + \epsilon \cos(\theta + \Upsilon)} \right]}{(k^2 - \epsilon^2)^{3/2}} \\
& + \frac{A_s \left(k^2 + \frac{\epsilon^2}{2} \right)}{(k^2 - \epsilon^2)^{5/2}} \cos^{-1} \left[\frac{\epsilon + k \cos(\theta + \Upsilon)}{k + \epsilon \cos(\theta + \Upsilon)} \right] \\
& + \frac{A_s \epsilon \sin(\theta + \Upsilon) [\epsilon^2 - 3\epsilon k \cos(\theta + \Upsilon) - 4k^2]}{2(k^2 - \epsilon^2)^2 [k + \epsilon \cos(\theta + \Upsilon)]^2} + B_s \quad (8)
\end{aligned}$$

where A and B are constants of integration.



(c)

The boundary conditions for the ridge and step regions can be written as (see sketch (c))

$$(1) P_{r, \infty} = 0 \quad \text{when} \quad \theta = \frac{2\pi(n-1)}{N} = \eta$$

where $n = 1, \dots, N$ and N is the number of steps placed around the bearing.

$$(2) P_{r, \infty} = P_{s, \infty} = P_c \quad \text{when} \quad \theta = \frac{2\pi}{N}(n-1 + \psi) = \sigma$$

where $\psi = \gamma/(\gamma + \beta + \delta)$.

$$(3) P_{s, \infty} = 0 \quad \text{when} \quad \theta = \frac{2\pi}{N}(n - \delta) = \xi$$

In order to avoid needless repetition, detailed analysis is hereinafter restricted to the step region. Substitution of boundary conditions (2) and (3) into equation (8) gives

$$P_{s, \infty} = \frac{\epsilon \sin(\theta + \Upsilon)}{(k^2 - \epsilon^2)[k + \epsilon \cos(\theta + \Upsilon)]} - \frac{k \cos^{-1} \left[\frac{\epsilon + k \cos(\theta + \Upsilon)}{k + \epsilon \cos(\theta + \Upsilon)} \right]}{(k^2 - \epsilon^2)^{3/2}} + G_s$$

$$+ \left(\frac{P_c - S_s - G_s}{T_s - J_s} \right) \left\{ -J_s + \frac{k^2 + \frac{\epsilon^2}{2}}{(k^2 - \epsilon^2)^{5/2}} \cos^{-1} \left[\frac{\epsilon + k \cos(\theta + \Upsilon)}{k + \epsilon \cos(\theta + \Upsilon)} \right] \right.$$

$$\left. + \frac{\epsilon \sin(\theta + \Upsilon) [\epsilon^2 - 3\epsilon k \cos(\theta + \Upsilon) - 4k^2]}{2(k^2 - \epsilon^2)^2 [k + \epsilon \cos(\theta + \Upsilon)]^2} \right\} \quad (9)$$

where

$$G_s = \frac{\epsilon \sin(\xi + \Upsilon)}{(k^2 - \epsilon^2)[k + \epsilon \cos(\xi + \Upsilon)]} + \frac{k}{(k^2 - \epsilon^2)^{3/2}} \cos^{-1} \left[\frac{\epsilon + k \cos(\xi + \Upsilon)}{k + \epsilon \cos(\xi + \Upsilon)} \right]$$

$$J_s = \frac{\left(\frac{k^2 + \epsilon^2}{2}\right)}{(k^2 - \epsilon^2)^{5/2}} \cos^{-1} \left[\frac{\epsilon + k \cos(\xi + \Upsilon)}{k + \epsilon \cos(\xi + \Upsilon)} \right] - \frac{\epsilon \sin(\xi + \Upsilon) [\epsilon^2 - 3\epsilon k \cos(\xi + \Upsilon) - 4k^2]}{2(k^2 - \epsilon^2)^2 [k + \epsilon \cos(\xi + \Upsilon)]^2}$$

$$S_s = \frac{\epsilon \sin(\sigma + \Upsilon)}{(k^2 - \epsilon^2) [k + \epsilon \cos(\sigma + \Upsilon)]} - \frac{k \cos^{-1} \left[\frac{\epsilon + k \cos(\sigma + \Upsilon)}{k + \epsilon \cos(\sigma + \Upsilon)} \right]}{(k^2 - \epsilon^2)^{3/2}}$$

$$T_s = \frac{\left(\frac{k^2 + \epsilon^2}{2}\right)}{(k^2 - \epsilon^2)^{5/2}} \cos^{-1} \left[\frac{\epsilon + k \cos(\sigma + \Upsilon)}{k + \epsilon \cos(\sigma + \Upsilon)} \right] + \frac{\epsilon \sin(\sigma + \Upsilon) [\epsilon^2 - 3\epsilon k \cos(\sigma + \Upsilon) - 4k^2]}{2(k^2 - \epsilon^2)^2 [k + \epsilon \cos(\sigma + \Upsilon)]^2}$$

The dimensionless pressure in the ridge region $P_{r, \infty}$ is written directly by making the following substitutions to the preceding equations

$$\left. \begin{array}{l} k \rightarrow 1 \\ \xi \rightarrow \eta \\ \text{Subscript } s \rightarrow \text{Subscript } r \end{array} \right\} \quad (10)$$

In order to solve for the dimensionless pressure at the common boundary P_c , it is necessary to equate the flow rate in the ridge and step regions (eqs. (3) and (4)) at the common boundary, which yields the following equation:

$$\left(H_r\right)_{\theta=\sigma} + \left(H_r^3 \frac{dP_{r, \infty}}{d\theta}\right)_{\theta=\sigma} = \left(H_s\right)_{\theta=\sigma} + \left(H_s \frac{dP_{s, \infty}}{d\theta}\right)_{\theta=\sigma}$$

Substitution of the dimensionless pressure while in the step and ridge regions into this equation gives the dimensionless pressure at the common boundary as

$$P_c = \frac{(T_s - J_s)(S_r + G_r) - (T_r - J_r)(S_s + G_s)}{(T_s - J_s) - (T_r - J_r)} \quad (11)$$

For each pad around the journal the dimensionless radial and tangential load components

in the step region can be written as

$$WR_{S, \infty} = \frac{wR_{S, \infty}}{p_a R \Gamma} = - \int_{\sigma}^{\xi} P_{S, \infty} \cos(\theta + \Upsilon) d\theta$$

$$WT_{S, \infty} = \frac{wt_{S, \infty}}{p_a R \Gamma} = \int_{\sigma}^{\xi} P_{S, \infty} \sin(\theta + \Upsilon) d\theta$$

Substitution of equation (9) into these equations gives

$$WR_{S, \infty} = \frac{\cos(\xi + \Upsilon) - \cos(\sigma + \Upsilon)}{k^2 - \epsilon^2} - \frac{kg_S}{(k^2 - \epsilon^2)^{3/2}} + G_S [\sin(\sigma + \Upsilon) - \sin(\xi + \Upsilon)]$$

$$+ \left(\frac{P_c - S_S - G_S}{T_S - J_S} \right) \left\{ S_S + \frac{g_S \left(k^2 + \frac{\epsilon^2}{2} \right)}{(k^2 - \epsilon^2)^{5/2}} + J_S [\sin(\xi + \Upsilon) - \sin(\sigma + \Upsilon)] \right\} \quad (12)$$

$$WT_{S, \infty} = \frac{\sin(\sigma + \Upsilon) - \sin(\xi + \Upsilon)}{k^2 - \epsilon^2} - \frac{\epsilon t_S + kr_S}{(k^2 - \epsilon^2)^{3/2}} + G_S [\cos(\sigma + \Upsilon) - \cos(\xi + \Upsilon)]$$

$$- \left(\frac{P_c - S_S - G_S}{T_S - J_S} \right) \left\{ J_S [\cos(\sigma + \Upsilon) - \cos(\xi + \Upsilon)] - \frac{1}{2(k^2 - \epsilon^2)} \left[\frac{\sin(\sigma + \Upsilon)}{k + \epsilon \cos(\sigma + \Upsilon)} \right. \right.$$

$$\left. \left. - \frac{\sin(\xi + \Upsilon)}{k + \epsilon \cos(\xi + \Upsilon)} \right] + \frac{3k [\sin(\sigma + \Upsilon) - \sin(\xi + \Upsilon)]}{2(k^2 - \epsilon^2)^2} - \frac{3\epsilon kt_S + 2r_S \left(k^2 + \frac{\epsilon^2}{2} \right)}{2(k^2 - \epsilon^2)^{5/2}} \right\} \quad (13)$$

where

$$\begin{aligned}
t_s &= \cos^{-1} \left[\frac{\epsilon + k \cos(\sigma + \Upsilon)}{k + \epsilon \cos(\sigma + \Upsilon)} \right] - \cos^{-1} \left[\frac{\epsilon + k \cos(\xi + \Upsilon)}{k + \epsilon \cos(\xi + \Upsilon)} \right] \\
g_s &= \sin(\sigma + \Upsilon) \cos^{-1} \left[\frac{\epsilon + k \cos(\sigma + \Upsilon)}{k + \epsilon \cos(\sigma + \Upsilon)} \right] - \sin(\xi + \Upsilon) \cos^{-1} \left[\frac{\epsilon + k \cos(\xi + \Upsilon)}{k + \epsilon \cos(\xi + \Upsilon)} \right] \\
s_s &= \frac{k[\cos(\sigma + \Upsilon) - \cos(\xi + \Upsilon)]}{2(k^2 - \epsilon^2)} \left\{ \frac{3}{k^2 - \epsilon^2} - \frac{1}{[k + \epsilon \cos(\sigma + \Upsilon)][k + \epsilon \cos(\xi + \Upsilon)]} \right\} \\
r_s &= \cos(\sigma + \Upsilon) \cos^{-1} \left[\frac{\epsilon + k \cos(\sigma + \Upsilon)}{k + \epsilon \cos(\sigma + \Upsilon)} \right] - \cos(\xi + \Upsilon) \cos^{-1} \left[\frac{\epsilon + k \cos(\xi + \Upsilon)}{k + \epsilon \cos(\xi + \Upsilon)} \right]
\end{aligned}$$

The dimensionless radial and tangential load components in the ridge region $WR_{r, \infty}$ and $WT_{r, \infty}$ can be written directly by making the following substitutions to the preceding equations

$$\left. \begin{aligned}
&k \rightarrow 1 \\
&\xi \rightarrow \sigma \\
&\sigma \rightarrow \eta \\
&\text{Subscript } s \rightarrow \text{Subscript } r
\end{aligned} \right\} \quad (14)$$

The total dimensionless radial and tangential loads of the Rayleigh step journal bearing can be written as

$$WR_{\infty} = \frac{wr_{\infty}}{p_a R \Gamma} = \sum_{n=1}^N (WR_{r, \infty} + WR_{s, \infty}) \quad (15)$$

$$WT_{\infty} = \frac{wt_{\infty}}{p_a R \Gamma} = \sum_{n=1}^N (WT_{r, \infty} + WT_{s, \infty}) \quad (16)$$

The total dimensionless load capacity and attitude angle for a Rayleigh step journal bearing are . . .

$$W_{\infty} = \frac{w_{\infty}}{p_a R \Gamma} = \left(WR_{\infty}^2 + WT_{\infty}^2 \right)^{1/2} \quad (17)$$

$$\Phi_{\infty} = \tan^{-1} \left(\frac{WT_{\infty}}{WR_{\infty}} \right) \quad (18)$$

The dimensionless load capacity and attitude angle of an infinite-length Rayleigh step journal bearing are functions of the following parameters:

- (1) Bearing parameters ϵ and Υ
- (2) Step parameters N , k , ψ , and δ

The equations for the shear stress at the moving member in the ridge and step regions can be written as

$$\tau_{r, \infty} = \frac{\mu U}{h_r} - \frac{h_r}{2R} \frac{dp_{r, \infty}}{d\theta}$$

$$\tau_{s, \infty} = \frac{\mu U}{h_s} - \frac{h_s}{2R} \frac{dp_{s, \infty}}{d\theta}$$

The friction force per unit length at the moving member in the ridge and step regions is then

$$f_{r, \infty} = R \int_{\eta}^{\sigma} \tau_{r, \infty} d\theta = \frac{\mu UR}{C_r} \left\{ \int_{\eta}^{\sigma} \frac{d\theta}{1 + \epsilon \cos(\theta + \Upsilon)} - 3 \int_{\eta}^{\sigma} [1 + \epsilon \cos(\theta + \Upsilon)] \frac{dP_{r, \infty}}{d\theta} d\theta \right\}$$

$$f_{s, \infty} = R \int_{\sigma}^{\xi} \tau_{s, \infty} d\theta = \frac{\mu UR}{C_r} \left\{ \int_{\sigma}^{\xi} \frac{d\theta}{k + \epsilon \cos(\theta + \Upsilon)} - 3 \int_{\sigma}^{\xi} [k + \epsilon \cos(\theta + \Upsilon)] \frac{dP_{s, \infty}}{d\theta} d\theta \right\}$$

Integration by parts gives the following

$$f_{r, \infty} = \frac{R\mu U}{C_r} \left\{ \frac{t_r}{\sqrt{1 - \epsilon^2}} - 3P_c [1 + \epsilon \cos(\sigma + \Upsilon)] - 3\epsilon WT_{r, \infty} \right\}$$

$$f_{s, \infty} = \frac{R\mu U}{C_r} \left\{ -\frac{t_s}{\sqrt{k^2 - \epsilon^2}} + 3P_c [k + \epsilon \cos(\sigma + \Upsilon)] - 3\epsilon WT_{s, \infty} \right\}$$

The total dimensionless friction force can be written as

$$F_{\infty} = \frac{C_r \sum_{n=1}^N (f_{r, \infty} + f_{s, \infty})}{2\pi R \mu U} = \frac{1}{2\pi} \sum_{n=1}^N \left\{ \frac{t_r}{\sqrt{1 - \epsilon^2}} - \frac{t_s}{\sqrt{k^2 - \epsilon^2}} + 3P_c (k - 1) - 3\epsilon (WT_{r, \infty} + WT_{s, \infty}) \right\} \quad (19)$$

DISCUSSION OF RESULTS

Numerical solutions of equations (9) to (19) were evaluated on a digital computer for a number of cases of interest. The angle subtended by the lubrication groove δ is 2° for all the data to be presented. Therefore, the load capacity, the attitude angle, and

TABLE I. - EFFECT OF STEP CONFIGURATIONS ON DIMENSIONLESS LOAD CAPACITY, ATTITUDE ANGLE, AND DIMENSIONLESS FRICTION FORCE

[Eccentricity ratio, 0.1000×10^{-15} ; radius to length ratio, 0.1000×10^{-15} ; number of steps, 1; shear stress, 0; angle subtended by lubrication groove, 2° .]

| Film thickness ratio, k | Dimensionless load capacity, W_∞ ; attitude angle, Φ_∞ ; dimensionless friction force, F_∞ | Ratio of angle subtended by ridge to angle subtended by pad, ψ | | | | | | | | |
|-------------------------|--|---|--------|--------|--------|--------|--------|--------|--------|--------|
| | | 0.10 | 0.20 | 0.30 | 0.35 | 0.40 | 0.45 | 0.50 | 0.70 | 0.99 |
| 1.01 | W_∞ | 0.0062 | 0.0117 | 0.0161 | 0.0177 | 0.0188 | 0.0195 | 0.0197 | 0.0157 | 0.0003 |
| 1.01 | Φ_∞ | 72.11 | 54.20 | 36.30 | 27.35 | 18.40 | 9.453 | .5024 | -35.30 | -87.21 |
| 1.01 | F_∞ | .9856 | .9866 | .9876 | .9881 | .9886 | .9891 | .9896 | .9916 | .9944 |
| 1.20 | W_∞ | .1158 | .2061 | .2663 | .2846 | .2950 | .2975 | .2928 | .2120 | .0033 |
| 1.20 | Φ_∞ | 72.11 | 54.20 | 36.30 | 27.35 | 18.40 | 9.453 | .5028 | -35.30 | -87.21 |
| 1.20 | F_∞ | .8554 | .8788 | .8993 | .9087 | .9176 | .9259 | .9339 | .9618 | .9940 |
| 1.40 | W_∞ | .2115 | .3500 | .4257 | .4430 | .4481 | .4421 | .4262 | .2879 | .0041 |
| 1.40 | Φ_∞ | 72.11 | 54.20 | 36.30 | 27.35 | 18.40 | 9.453 | .5027 | -35.30 | -87.21 |
| 1.40 | F_∞ | .7756 | .8242 | .8619 | .8778 | .8921 | .9050 | .9168 | .9550 | .9940 |
| 1.50 | W_∞ | .2508 | .3997 | .4731 | .4868 | .4875 | .4766 | .4557 | .3001 | .0042 |
| 1.50 | Φ_∞ | 72.11 | 54.20 | 36.30 | 27.35 | 18.40 | 9.453 | .5027 | -35.30 | -87.21 |
| 1.50 | F_∞ | .7507 | .8107 | .8545 | .8723 | .8880 | .9020 | .9146 | .9545 | .9939 |
| 1.60 | W_∞ | .2843 | .4368 | .5039 | .5132 | .5094 | .4942 | .4693 | .3026 | .0041 |
| 1.60 | Φ_∞ | 72.11 | 54.20 | 36.30 | 27.35 | 18.40 | 9.453 | .5027 | -35.30 | -87.21 |
| 1.60 | F_∞ | .7331 | .8029 | .8510 | .8700 | .8865 | .9011 | .9140 | .9544 | .9939 |
| 1.68 | W_∞ | .3064 | .4578 | .5185 | .5243 | .5173 | .4992 | .4720 | .3002 | .0040 |
| 1.68 | Φ_∞ | 72.11 | 54.20 | 36.30 | 27.35 | 18.40 | 9.453 | .5027 | -35.30 | -87.21 |
| 1.68 | F_∞ | .7233 | .7994 | .8499 | .8694 | .8862 | .9010 | .9140 | .9544 | .9939 |
| 1.70 | W_∞ | .3121 | .4627 | .5214 | .5263 | .5184 | .4996 | .4717 | .2989 | .0040 |
| 1.70 | Φ_∞ | 72.11 | 54.20 | 36.30 | 27.35 | 18.40 | 9.453 | .5028 | -35.30 | -87.21 |
| 1.70 | F_∞ | .7210 | .7988 | .8497 | .8693 | .8862 | .9010 | .9140 | .9544 | .9939 |
| 1.80 | W_∞ | .3345 | .4792 | .5287 | .5295 | .5181 | .4965 | .4665 | .2914 | .0039 |
| 1.80 | Φ_∞ | 72.11 | 54.20 | 36.30 | 27.35 | 18.40 | 9.453 | .5027 | -35.30 | -87.21 |
| 1.80 | F_∞ | .7131 | .7969 | .8495 | .8693 | .8862 | .9009 | .9139 | .9540 | .9939 |
| 1.90 | W_∞ | .3519 | .4880 | .5282 | .5254 | .5111 | .4875 | .4561 | .2816 | .0037 |
| 1.90 | Φ_∞ | 72.11 | 54.20 | 36.30 | 27.35 | 18.40 | 9.453 | .5027 | -35.30 | -87.21 |
| 1.90 | F_∞ | .7083 | .7964 | .8494 | .8692 | .8860 | .9005 | .9133 | .9533 | .9939 |
| 2.00 | W_∞ | .3647 | .4906 | .5219 | .5160 | .4996 | .4745 | .4425 | .2705 | .0035 |
| 2.00 | Φ_∞ | 72.11 | 54.20 | 36.30 | 27.35 | 18.40 | 9.453 | .5027 | -35.30 | -87.21 |
| 2.00 | F_∞ | .7056 | .7963 | .8492 | .8687 | .8852 | .8996 | .9122 | .9521 | .9939 |
| 2.20 | W_∞ | .3785 | .4821 | .4984 | .4880 | .4687 | .4423 | .4101 | .2469 | .0032 |
| 2.20 | Φ_∞ | 72.11 | 54.20 | 36.30 | 27.35 | 18.40 | 9.453 | .5027 | -35.30 | -87.21 |
| 2.20 | F_∞ | .7038 | .7959 | .8471 | .8658 | .8818 | .8958 | .9083 | .9488 | .9938 |
| 2.40 | W_∞ | .3799 | .4620 | .4670 | .4539 | .4334 | .4070 | .3759 | .2239 | .0029 |
| 2.40 | Φ_∞ | 72.11 | 54.20 | 36.30 | 27.35 | 18.40 | 9.453 | .5027 | -35.30 | -87.21 |
| 2.40 | F_∞ | .7037 | .7935 | .8424 | .8604 | .8760 | .8898 | .9023 | .9442 | .9937 |
| 2.60 | W_∞ | .3728 | .4361 | .4331 | .4185 | .3978 | .3722 | .3428 | .2025 | .0026 |
| 2.60 | Φ_∞ | 72.11 | 54.20 | 36.30 | 27.35 | 18.40 | 9.453 | .5027 | -35.30 | -87.21 |
| 2.60 | F_∞ | .7030 | .7887 | .8352 | .8528 | .8681 | .8820 | .8947 | .9389 | .9937 |
| 3.00 | W_∞ | .3438 | .3793 | .3673 | .3522 | .3327 | .3098 | .2842 | .1661 | .0021 |
| 3.00 | Φ_∞ | 72.11 | 54.20 | 36.30 | 27.35 | 18.40 | 9.453 | .5027 | -35.30 | -87.21 |
| 3.00 | F_∞ | .6968 | .7726 | .8158 | .8329 | .8486 | .8631 | .8768 | .9270 | .9935 |

the friction force of an infinite-length Rayleigh step journal bearing are functions of the bearing parameters (the eccentricity ratio ϵ and eccentricity orientation angle Υ), as well as of the step parameters (the number of steps placed around the journal N , the film thickness ratio k , and the ratio of the angle subtended by the ridge to the angle subtended by the pad ψ).

Table I and table I of reference 1 show that the dimensionless load capacity, friction force, and attitude angle obtained from the infinite-length bearing solution ($\zeta = 0$) for the case $\epsilon = 0$ approach the values obtained from the zero-order perturbation solution ($\epsilon = 0$) for the case $\zeta = 0$.

Figure 1 shows the effect of the number of steps placed around the journal on the dimensionless load capacity for various eccentricity ratios. A significant decrease in load capacity is evident as the number of steps is increased. For an eccentricity ratio of 0.1 the two-step bearing has only 20 percent of the load capacity of the one-step bearing; the three-step bearing has only 9 percent. From this figure it is evident that a one-step Rayleigh step journal is optimal when considering load capacity. Data obtained for other step configurations produced results similar to those shown in this figure.

Figures 2 and 3 show the effects of the step configuration on the dimensionless load capacity for various eccentricity ratios. In both figures it is apparent that, for $\epsilon \geq 0.2$, the optimal configuration when load capacity is considered tends toward the Sommerfeld bearing (i. e., $k = 1$ or $\psi = 1$). Figure 2 shows that, for small eccentricity ratios ($\epsilon < 0.2$) and $\psi = 0.45$, an optimal film thickness ratio k of 1.7 exists. Figure 3 shows that, for small eccentricity ratios and $k = 1.7$, the optimal step location varies with eccentricity ratio. This indicates that at low eccentricity ratios ($\epsilon < 0.2$) the pressure buildup at the common boundary is much more effective than when the bearing is operating at larger eccentricity ratios ($\epsilon \geq 0.2$).

The hypothesis that a fluid film bearing whose attitude angle is small is a stable bearing, as put forth by Gunter (ref. 5), is used in this report. That is, in a fluid film bearing, it is the tangential load component that generates the force required to initiate whirl instability. The attitude angle is a direct measure of the ratio of the tangential force to the radial force, and hence, is a direct measure of the relative stability of the bearing.

Figures 4 and 5 show the effect of eccentricity ratio on dimensionless load capacity and attitude angle for various values of the step-location parameter ψ . Therefore, making use of the hypothesis of Gunter (ref. 5) as well as of figures 4 and 5 results in the following optimal step parameters:

- (1) $\psi = 0.5$, optimal bearing when load capacity is considered
- (2) $\psi = 0.4$, optimal bearing when attitude angle is considered
- (3) $\psi = 0.45$, optimal bearing when both load capacity and attitude angle are considered

Final choice would depend on whether load capacity, stability, or both load capacity and stability is more important in the application being considered.

Thus far in the data presented, the eccentricity orientation angle has been fixed at 0° . For a better physical understanding of what is meant by eccentricity orientation angle figures 6 and 7 are presented. These figures illustrate the Sommerfeld and Rayleigh step journal bearing for eccentricity orientation angles of 0 , $\pi/2$, π , and $3\pi/2$. These figures also show the orientation of the attitude angle Φ .

Figure 8 shows the effect of eccentricity orientation angle on dimensionless load capacity for various eccentricity ratios ϵ . For $\epsilon = 0.1$ there are slight variations in load capacity as the eccentricity orientation angle is varied. However, for eccentricity ratios of 0.3 , 0.5 , 0.7 , and 0.9 there is a substantial decrease in load capacity when $\Upsilon = 270^\circ$. Figure 9 shows the effect of eccentricity orientation angle on attitude angle for various eccentricity ratios. For eccentricity ratios of 0.1 and 0.3 , when the eccentricity orientation angle changes, the attitude angle changes accordingly so that the resulting load acts through the location of the step. For higher eccentricity ratios ($\epsilon = 0.5, 0.7, 0.9$) the step is less effective.

Figures 10 and 11 show the effect of eccentricity orientation angle on midplane pressure distribution of both a Rayleigh step and a Sommerfeld journal bearing for eccentricity ratios of 0.1 and 0.5 . Figure 10 shows that for a eccentricity ratio of 0.1 the pressure buildup caused by the step is significant and positive completely around the bearing, whereas for $\Upsilon = 3\pi/2$ the Sommerfeld bearing has negative pressures completely around the bearing. This is because the maximum pressure is 90° out of phase with the location of minimum film thickness. For $\Upsilon = 3\pi/2$ the maximum pressure is at $\theta = 360^\circ$. However at $\theta = 360^\circ$ the pressure is ambient; therefore, the pressure is negative anywhere other than at 360° .

Earlier it was shown that as the eccentricity ratio increases the step becomes less effective and acts as a Sommerfeld bearing. From figure 11 it is evident that there is essentially no pressure buildup for $\Upsilon = 3\pi/2$ for the Rayleigh step journal bearing. The reason for this is that for $\Upsilon = 3\pi/2$ and $\epsilon = 0.5$ the positive pressure buildup caused by the step is offset by the negative pressure generated as the Rayleigh step journal adopts characteristics of the Sommerfeld bearing. This explains the load depression shown in figure 8 for $\epsilon = 0.5$ and $\Upsilon = 3\pi/2$.

Finally, it should be pointed out that the theoretical negative pressure region of the Sommerfeld bearing (see figs. 10 and 11) contributes to a positive load. In actuality this is not true, as is pointed out in reference 6. However, the Rayleigh step journal bearing contains a positive pressure completely or almost completely around the bearing. Therefore, the theoretical load capacity of the Rayleigh step journal bearing compares realistically to actual experiments, whereas the Sommerfeld bearing experiments show load capacity considerably lower than the theoretical value (ref. 6).

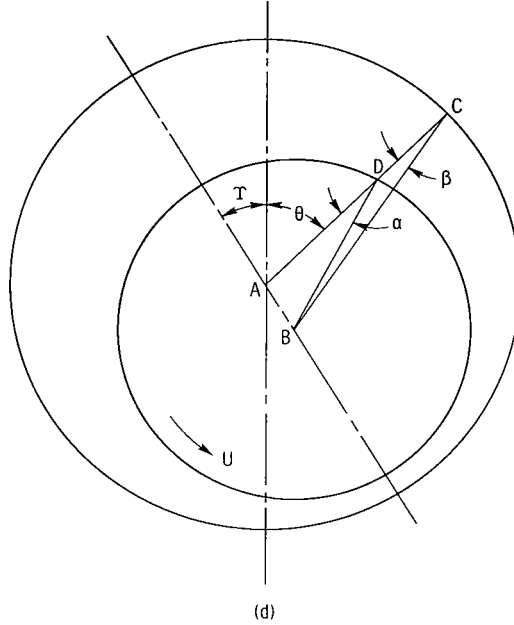
CONCLUSIONS

An analysis of an infinite-length Rayleigh step journal bearing was performed. The resulting expressions for dimensionless pressure, load, friction, and attitude angle were evaluated on a digital computer. The results indicated that one step placed around the journal was optimal. For eccentricity ratios greater than or equal to 0.2 the maximum load occurred for the Sommerfeld bearing, or one without a step. For eccentricity ratios less than 0.2 the optimal film thickness of 1.7 was found, while there were three optimal ratios of the angle subtended by the ridge to the angle subtended by the pad of 0.4, 0.45, and 0.5. These ratios depend on whether load capacity, or stability, or both load capacity and stability is more important in the application being considered. It also was determined from pressure profiles for various eccentricity orientation angles that the optimal Rayleigh step journal bearing is superior to the conventional Sommerfeld bearing.

Lewis Research Center,
National Aeronautics and Space Administration,
Cleveland, Ohio, August 8, 1968,
120-27-04-22.

APPENDIX - DERIVATION OF FILM THICKNESS EQUATION

Sketch (d) shows the eccentric journal with the coordinate orientation used for the Rayleigh step journal bearing. The equation for the film thickness h_r , defined as the distance from D to C in sketch (d) is derived herein. The following equalities are given $e = AB$, $BD = R$, $AC = R + C_r$ along with the angles θ and Υ . Therefore, the problem is to express h_r in terms of θ , Υ , e , R , and C_r .



From the triangle ABD the following equations can be written:

$$\sin \alpha = \frac{e}{R} \sin(\theta + \Upsilon) \quad (\text{A1})$$

therefore,

$$\cos \alpha = \sqrt{1 - \frac{e^2}{R^2} \sin^2(\theta + \Upsilon)} \approx 1 \quad (\text{A2})$$

From the triangle BCD the following equations can be written which make use of equations (A1) and (A2)

$$BC = \frac{e \sin(\theta + \Upsilon)}{\sin \beta} \quad (\text{A3})$$

$$h_r = e \sin(\theta + \Upsilon) \text{ctn } \beta - R \quad (\text{A4})$$

From the triangle ABC the following equation can be written:

$$BC = \frac{(R + C_r) \sin(\theta + \Upsilon)}{\sin(\theta + \Upsilon - \beta)} \quad (\text{A5})$$

Therefore, from equations (A3) and (A5) the following equation can be written:

$$\text{ctn } \beta = \frac{R + C_r + e \cos(\theta + \Upsilon)}{e \sin(\theta + \Upsilon)}$$

Substituting this into equation (A4) gives

$$h_r = C_r + e \cos(\theta + \Upsilon) \quad (\text{A6})$$

REFERENCES

1. Hamrock, Bernard J.; and Anderson, William J.: Incompressibly Lubricated Rayleigh Step Journal Bearing. I - Zero-Order Perturbation Solution. NASA TN D-4839, 1968.
2. Lord Rayleigh: Notes on the Theory of Lubrication. Phil. Mag., vol. 35, Jan. 1918, pp. 1-12.
3. Archibald, F. R.: A Simple Hydrodynamic Thrust Bearing. Trans. ASME, vol. 72, no. 4, May 1950, pp. 393-400.
4. Archibald, Frank R.: The Stepped Shape Film Applied to a Journal Bearing. J. Franklin Inst., vol. 253, no. 1, Jan. 1952, pp. 21-27.
5. Gunter, Edgar J., Jr.: Dynamic Stability of Rotor-Bearing Systems. NASA SP-113, 1966, p. 21.
6. Pinkus, Oscar; and Sternlicht, Beno: Theory of Hydrodynamic Lubrication. McGraw-Hill Book Co., Inc., 1961.

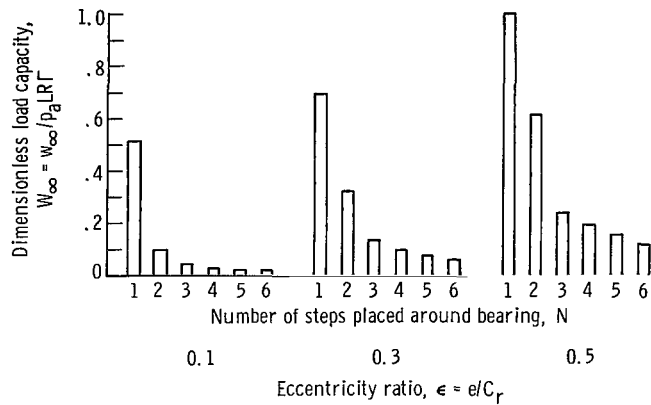


Figure 1. - Effect of number of steps placed around journal on dimensionless load capacity for eccentricity ratios of 0.1, 0.3, and 0.5. Film thickness ratio, 1.7; ratio of angle subtended by ridge to angle subtended by pad, 0.45; angle subtended by lubrication groove, 2° ; eccentricity orientation angle, 0° .

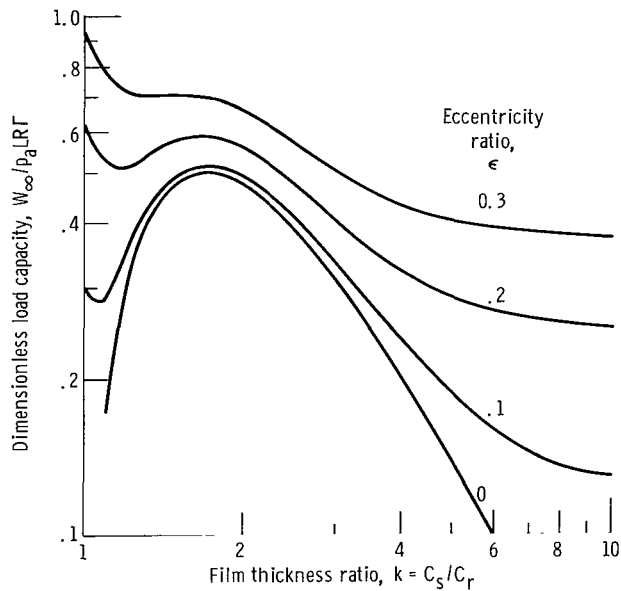


Figure 2. - Effect of film thickness ratio on dimensionless load capacity for eccentricity ratios of 0, 0.1, 0.2, and 0.3. Number of steps placed around bearing, 1; ratio of angle subtended by ridge to angle subtended by pad, 0.45; eccentricity orientation angle, 0° ; angle subtended by lubrication groove, 2° .

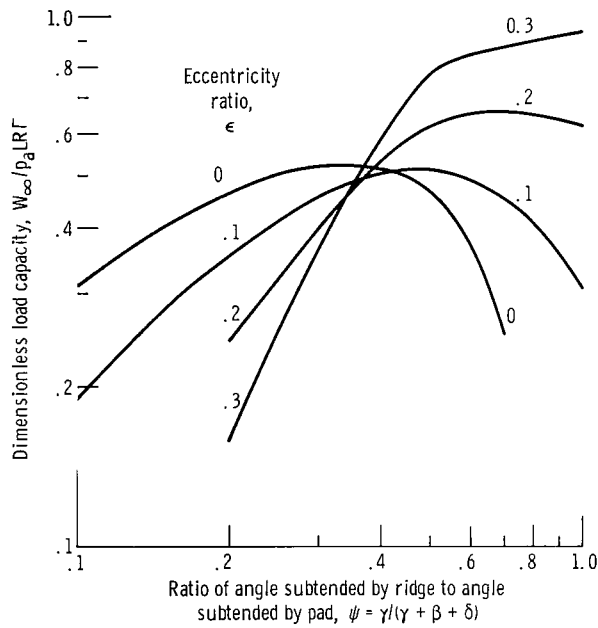


Figure 3. - Effect of step location on dimensionless load capacity for various values of eccentricity ratio. Number of steps placed around bearing, 1; eccentricity orientation angle, 0° ; angle subtended by lubrication groove, 2° ; film thickness ratio, 1.7.

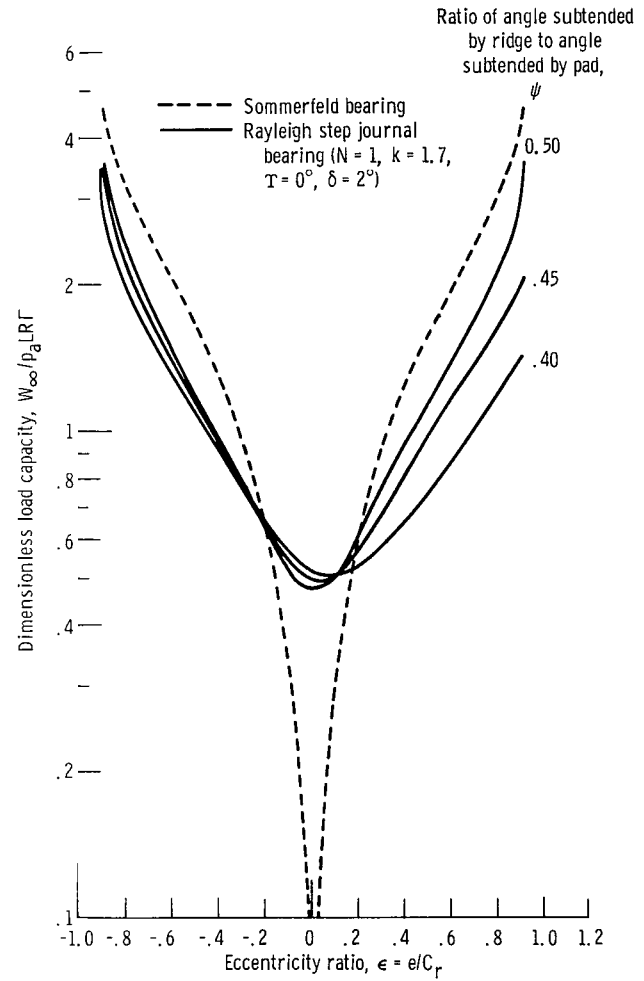


Figure 4. - Dimensionless load capacity as function of eccentricity ratio for Sommerfeld and Rayleigh step journal bearings.

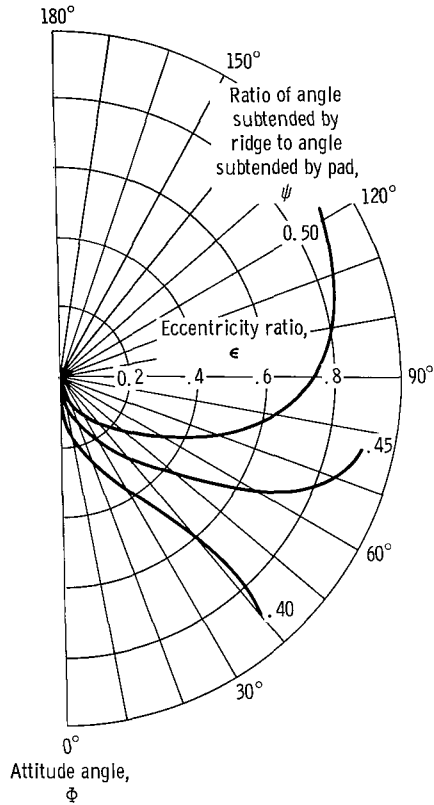


Figure 5. - Attitude angle as function of eccentricity ratio for three values of ratio of angle subtended by ridge to angle subtended by pad. Number of steps placed around bearing, 1; eccentricity orientation angle, 0° ; angle subtended by lubrication groove, 2° ; film thickness ratio, 1.7.

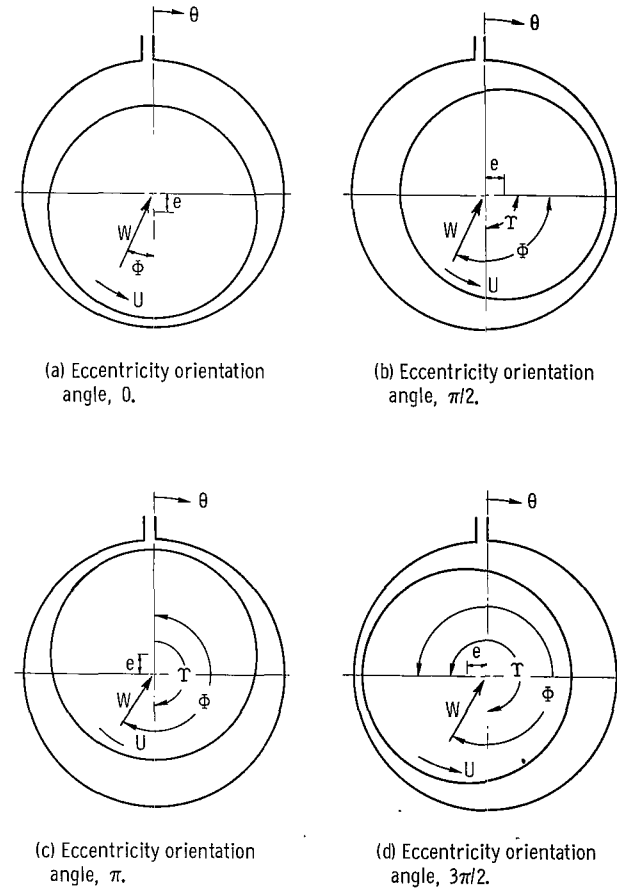


Figure 6. - Illustration of Sommerfeld bearing for eccentricity orientation angles of $0, \pi/2, \pi$, and $3\pi/2$.

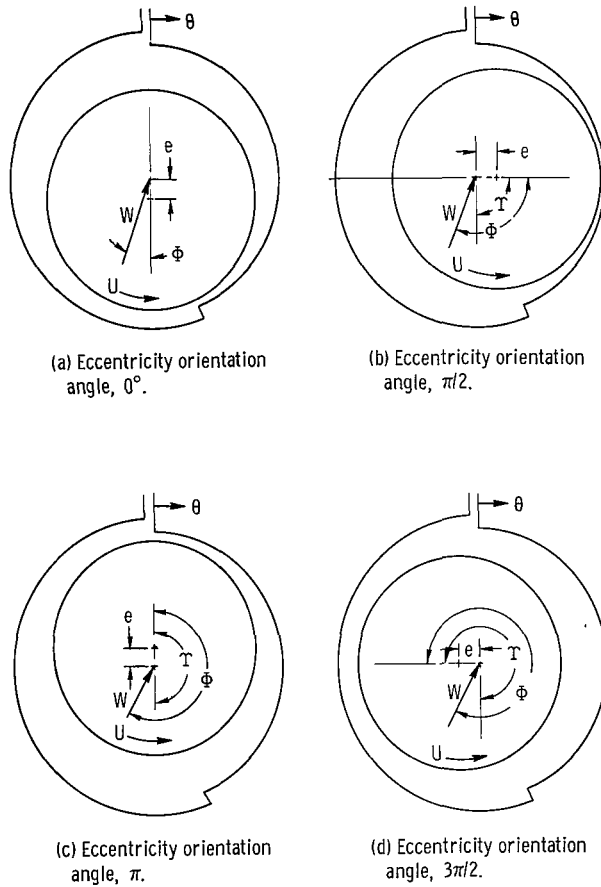


Figure 7. - Illustration of Rayleigh step journal bearing for eccentricity orientation angles of 0 , $\pi/2$, π , and $3\pi/2$.

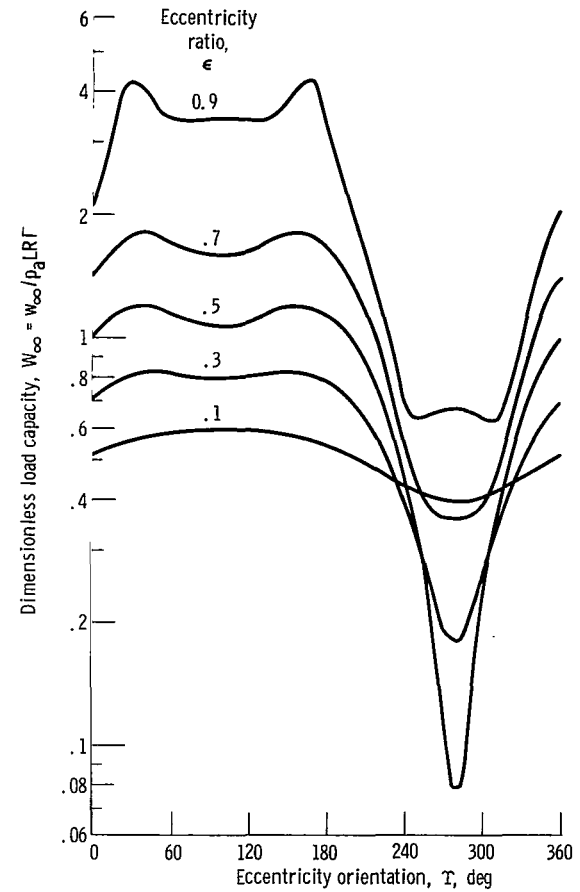


Figure 8. - Effect of eccentricity orientation angle on dimensionless load capacity for eccentricity ratios of 0.1 , 0.3 , 0.5 , 0.7 , and 0.9 . Number of steps placed around bearing, 1 ; ratio of angle subtended by ridge to angle subtended by pad, 0.45 ; angle subtended by lubrication groove, 2° ; film thickness ratio, 1.7 .

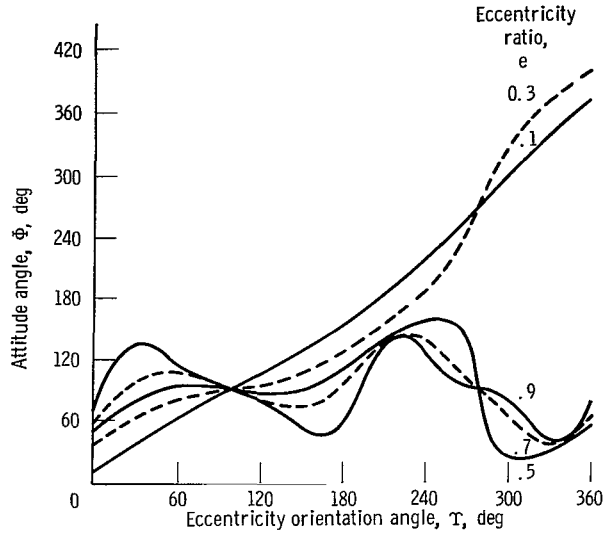


Figure 9. - Effect of eccentricity orientation angle on attitude angle for eccentricity ratios of 0.1, 0.3, 0.5, 0.7, and 0.9. Number of steps placed around bearing, 1; ratio of angle subtended by ridge to angle subtended by pad, 0.45; angle subtended by lubrication groove, 2°; film thickness ratio, 1.7.

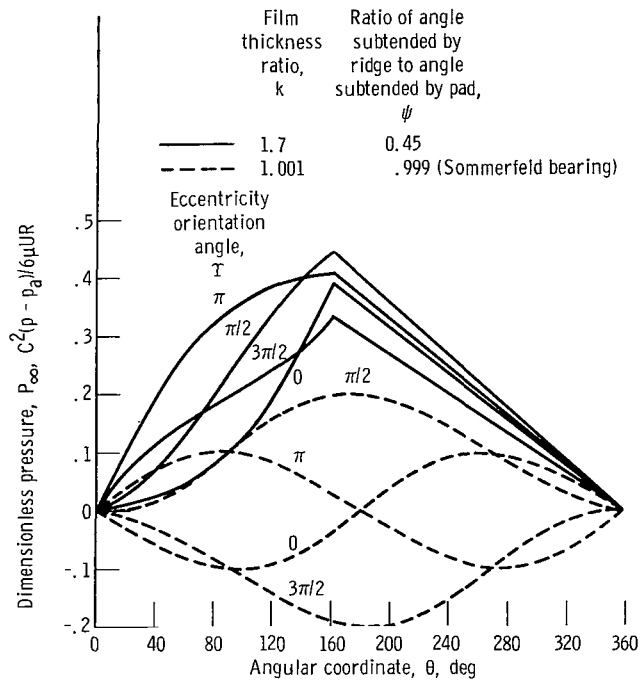


Figure 10. - Effect of eccentricity orientation angle on midplane pressure distribution of a Rayleigh and a Sommerfeld bearing for eccentricity ratio of 0.1. Number of steps placed around bearing, 1; angle subtended by lubrication groove, 2°.

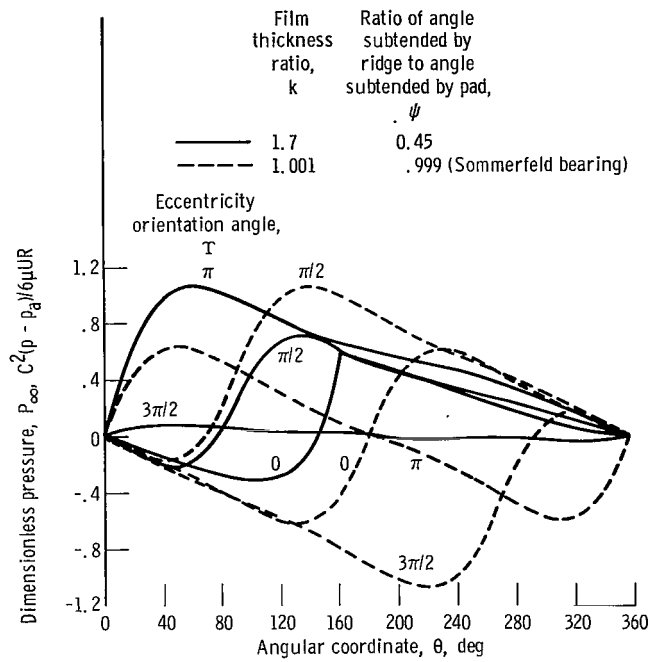


Figure 11. - Effect of eccentricity orientation angle on midplane pressure distribution of a Rayleigh step and a Sommerfeld bearing for eccentricity ratio of 0.1. Number of steps placed around bearing, 1; angle subtended by lubrication groove, 2° .

FIRST CLASS MAIL

POSTMASTER: If Undeliverable (Section 158
Postal Manual) Do Not Return

"The aeronautical and space activities of the United States shall be conducted so as to contribute . . . to the expansion of human knowledge of phenomena in the atmosphere and space. The Administration shall provide for the widest practicable and appropriate dissemination of information concerning its activities and the results thereof."

—NATIONAL AERONAUTICS AND SPACE ACT OF 1958

NASA SCIENTIFIC AND TECHNICAL PUBLICATIONS

TECHNICAL REPORTS: Scientific and technical information considered important, complete, and a lasting contribution to existing knowledge.

TECHNICAL NOTES: Information less broad in scope but nevertheless of importance as a contribution to existing knowledge.

TECHNICAL MEMORANDUMS: Information receiving limited distribution because of preliminary data, security classification, or other reasons.

CONTRACTOR REPORTS: Scientific and technical information generated under a NASA contract or grant and considered an important contribution to existing knowledge.

TECHNICAL TRANSLATIONS: Information published in a foreign language considered to merit NASA distribution in English.

SPECIAL PUBLICATIONS: Information derived from or of value to NASA activities. Publications include conference proceedings, monographs, data compilations, handbooks, sourcebooks, and special bibliographies.

TECHNOLOGY UTILIZATION PUBLICATIONS: Information on technology used by NASA that may be of particular interest in commercial and other non-aerospace applications. Publications include Tech Briefs, Technology Utilization Reports and Notes, and Technology Surveys.

Details on the availability of these publications may be obtained from:

SCIENTIFIC AND TECHNICAL INFORMATION DIVISION
NATIONAL AERONAUTICS AND SPACE ADMINISTRATION
Washington, D.C. 20546